A Simple Biofuel Cell Cathode with Human Red Blood Cells as Electrocatalysts for Oxygen Reduction Reaction

Yusuke Ayato [a,b,*], Kenichiro Sakurai [a], Saori Fukunaga [a], Takuya Suganuma [a], Kiyofumi Yamagiwa [a], Hidenobu Shiroishi [c], Jun Kuwano [a]

[a] Department of Industrial Chemistry, Faculty of Engineering, Tokyo University of Science, 12-1 Ichigaya-Funagawara-machi, Shinjyuku-ku, Tokyo 162-0826, Japan

[b] Present address: Faculty of Textile Science and Technology, Materials and Chemical Engineering, Shinshu University, 3-15-1 Tokida, Ueda, Nagano 386-8567, Japan

[c] Department of Chemical Science and Engineering, Tokyo National College of Technology, 1220-1 Kunugida-machi, Hachioji, Tokyo 193-0997, Japan

* Corresponding author at: Shinshu University Faculty of Textile Science and Technology, Materials and Chemical Engineering, Shinshu University, 3-15-1 Tokida, Ueda, Nagano 386-8567, Japan.

Tel: +81 268 21 5455; fax: +81 268 21 5452.

E-mail address: y-ayato@shinshu-u.ac.jp (Y. Ayato).

Keywords:

Biofuel Cell

Direct electron transfer

Oxygen reduction reaction

Red blood cell

Hemoglobin

Indium-tin-oxide (ITO) electrode

ABSTRACT

A red blood cell (RBC) from human exhibited direct electron transfer (DET) activity on a bare indium tin oxide (ITO) electrode. A formal potential of -0.15_2 V vs. a silver-silver chloride saturated potassium chloride (Ag|AgCl|KCl(satd.)) was estimated for the human RBC (type AB) from a pair of redox peaks at around 0.08_9 and -0.21_5 V (vs. Ag|AgCl|KCl(satd.)) on cyclic voltammetric (CV) measurements in a phosphate buffered saline (PBS; 39mM; pH 7.4) solution. The results agreed well with those of a redox couple for iron-bearing heme groups in hemoglobin molecules (HbFe(II)/HbFe(III)) on the bare ITO electrodes, indicated that DET active species were hemoglobin (Hb) molecules encapsulated by a phospholipid bilayer membrane of the human RBC. The quantity of electrochemically active Hb in the human RBC was estimated to be 30 pmol cm^{-2}. In addition, the human RBC exhibited oxygen reduction reaction (ORR) activity in the dioxygen (O_2) saturated PBS solution at the negative potential from *ca.* -0.15 V (vs. Ag|AgCl|KCl(satd.)). A single cell test proved that a biofuel cell (BFC) with an O_2|RBC|ITO cathode showed the open-circuit voltage (OCV) of *ca.* 0.43 V and the maximum power density of *ca.* 0.68 μW cm^{-2}.

1. Introduction

Biofuel cells (BFCs) are promising candidates for body implantable power supplies applied to medical devices such as pacemakers for cardiac resynchronization therapy (CRT) and deep brain stimulation (DBS), since the systems operate under mild conditions at around body temperature at near-neutral pHs as well as natural materials, e.g. glucose as the fuel and enzymes as the electrocatalysts, can be utilized at the electrode (Halámková et al., 2012; Zebda et al., 2009; Nazaruk et al., 2008; Togo et al., 2008). Various kinds of enzyme proteins, such as families of dehydrogenases, oxidases, peroxidases, etc., have been examined as the electrocatalysts both of the anode and the cathode, thus, the fuel cell reaction proceeds via a wide variety of the chemical reaction and the electron transfer process at the electrode in the field of BFCs (Rasmussen et al., 2012; Prakash et al., 2009; Drobov et al., 2008; Brunel et al., 2007; Kamitaka et al., 2007; Ikeda and Kano, 2003; Tsujimura et al., 2001; Katz et al., 1999; Gorton et al. 1999; Palmore et al., 1998).

The electrode reaction process of BFCs using enzyme proteins can be broadly classified into two types of mediated electron transfer (MET) and direct electron transfer (DET). According this, BFCs have been defined as follows. 1. DET-type BFCs: the systems where the electrons tunnel directly between the electrode and the active sites in enzymes, or transfer through the conductive part in the case that the individual enzyme has the electron carrying sites beside the reaction active sites. 2. MET-type BFCs: the systems based on other all electrode reactions involving electron transfer by using mediators and promoters (Ikeda and Kano, 2003; Bullen et al., 2006). It has been believed that most of the enzyme proteins acting as the electrocatalysts of fuel cell reactions show slow electron transfer characteristics on the simple DET-type electrode; hence, great efforts have been mainly made on the MET-type including modified and immobilized electrodes to enhance the enzyme activity (Yong et al., 2012; Cai et al. 2012; Kang et al., 2009). However, the simple DET-type electrode is the best design for the application to the body implantable power supplies, because of rejection to extracorporeal materials, necessity of purification, modification, and immobilization of enzymes onto the electrodes, etc. In addition, since the potential range for the BFC based on DET is generally close to the redox potential of the enzyme itself, it can be expected a high power-output compared with the MET-type BFCs.

Hemoglobin (Hb) is typically known as a tetrameric heme protein composed of two α-globin and two β-globin polypeptides, each of which includes one iron-bearing heme group. The four heme groups are located relatively near the surface of the protein shell the same as the family of peroxidases (Jones et al, 2012; Chen et al., 2009; Scheller et al., 2005; Perutz et al., 1968). In the Hb electrochemistry, it has been believed that the strong adsorption of proteins onto the electrode surfaces brought about a denaturation of the protein structure and slow electron transfer characteristics with the electrodes. Thus, the electrochemical investigations have been mainly performed with adding of mediators and promoters or modified and immobilized electrodes, i.e. by the MET types (Kafi and Crossley, 2013; Yin et al., 2005; Revenga-Parra et al., 2005; Topoglidis et al., 2003; Kawahara and Ohno, 1998; Shan et al., 2007; Shi et al., 2007; Zhao et al., 2006; Feng et al., 2006; Zhang and Oyama, 2004; Jia et al., 2004; Sun and Hu, 2004; Gu et al., 2001). On the other hand, we have demonstrated a simplest DET between Hb molecules and bare indium-tin-oxide (ITO) electrodes and found that the protein structure of Hb molecules on the bare ITO electrode surface should be similar to its own native state the same as that in the solution phase (Ayato et al., 2008; Ayato et al., 2007). Recently, we have developed a novel BFC cathode based on the simplest DET of the Hb molecules, reducing hydrogen peroxide (H_2O_2) to water, on the bare ITO electrodes

(Ayato and Matsuda, 2009). On the other hand, effort has been disclosed the electrocatalytic activity for dioxygen (O_2) reduction by Hb at some mediated, modified or immobilized electrodes (Zhao et al. 2007; Mimica et al., 2004; Zhou et al., 2002).

It is well-known that red blood cells (RBCs) are contained 45% in blood of human and transport O_2 to the whole body with Hb encapsulated by phospholipid bilayer membrane. The development of simple O_2 reduction cathode by utilizing RBCs enables us to practically apply to the body implantable power supplies because of unnecessary for the purification of the enzyme, immobilization or modification of the electrodes, construction of gas supplying systems, and considering the lifetime of enzymes, etc. However, so little reports included electron transfer characteristics of Hb in RBC with the electrodes even in recent years (Wang et al., 2010; Xu et al., 2008; Ci et al., 1998). In this study, we successfully observed not only the DET activity between RBCs encapsulating Hb and the bare ITO electrodes but also the electrocatalytic activity for O_2 reduction reaction (ORR) by Hb in RBC. In addition, single cell performance was evaluated by using O_2|RBC|ITO cathode and H_2|Pt/C anode.

2. Experimental section

2.1. Chemicals

RBCs from human group AB treated with glutaraldehyde (4%(m/m) RBCs suspended in phosphate buffered saline; PBS) and 39 mM PBS (pH 7.4) were purchased from Sigma and Kanto Chemical Co., Inc., respectively. Bovine Hb was purchased from SIGMA. All chemicals were used as received. Electrochemical glass cells and apparatus made by fluorocompound were soaked in 50:50 of sulfuric acid and nitric acid (Wako pure chemical industries, Ltd.) mixture at least for overnight and washed with Milli-Q water (resistance > 18 MΩcm).

2.2. Spectroscopic observations of human Hb in RBC and bovine Hb

UV-vis transmission spectra were observed on a UV-vis spectrophotometer of UV-2450 (Shimadzu). Reference spectra were observed in the PBS solution only before sample measurements. Concentrations of Hb and RBC solutions were adjusted to 31 μg ml^{-1} using the PBS solution. Sample spectra were observed in the prepared PBS solution containing RBC or Hb under the same conditions with reference measurements.

An optical image was obtained by a confocal laser scanning microscopy (CLSM) of LSM710 (Carl Zeiss Microscopy Co., Ltd.). The RBC solution was used as received and dropped on the ITO-coated glass plate (5Ω/sq., 330 nm thick; Geomatic Co. Ltd.) surface. Then, a cover glass was put on the RBC solution dispersed ITO-coated glass plate. The CLSM observation was carried out with a lens that magnifies 400 diameters.

2.3. Electrochemical characterizations of human RBC on bare ITO electrodes

The DET and the ORR activities of RBCs were investigated in a typical three-electrode electrochemical system. The ITO, a platinum (Pt) wire, and a silver-silver chloride saturated potassium chloride (Ag|AgCl|KCl(satd.)) were used as a working, counter, and reference electrodes, respectively. All potentials are quoted against the Ag|AgCl|KCl(satd.) electrode in this paper. Cyclic voltammetric (CV) measurements were performed in the PBS solutions containing and not containing 4% RBC at the bare ITO electrodes with the sweep rate from 0.01 to 10 V s^{-1}. The electrode potential was swept between +0.3 and -0.45 V. The CV curves were also recorded in O_2 saturated PBS solutions containing and not containing 4% RBC with the sweep rate of 0.01 V s^{-1}.

2.4. Performance of a single cell with O_2|RBC|ITO bio-cathode.

Figure S1 shows the construction of the single cell. A Pt dispersed carbon paper (1 mg cm^{-2} Pt loading, 20 %(m/m) Pt/Vulcan XC72, ElectroChem, Inc.) and ITO electrodes were used as the anode and cathode, respectively. Nafion® 117 membrane was employed to maintain ion transport and prevent the penetration of RBC to the anode. To purify and exchange with H^+, the Nafion membrane with 20 × 20 mm was soaked in 3%(m/m) H_2O_2 solution and boiled for 1 h, then stored in dilute H_2SO_4 solution. Membrane-electrode assemblies (MEA) were prepared by hot-pressing one Pt dispersed carbon paper and one Nafion® membrane. The pretreated Nafion membrane was soaked with water and dried at room temperature for 1 h. The Pt dispersed carbon paper was cut into 15 × 15 mm. The Pt dispersed surface of the carbon paper was covered with 80 μl of 5 %(m/m) Nafion® solution (SIGMA-Aldrich, Inc.), and pinched with Nafion membrane between two Teflon sheets, then hot-pressed for 2 min at 408 K. The carbon paper side of the prepared MEA was set on the single cell anode facing to a center hole with 10 mm in diameter as shown in Fig. S1. H_2 gas could be provided to the backside of the Pt dispersed carbon paper similarly to the polymer electrolyte fuel cells (Ayato et al., 2006; Ayato et al., 2003). The ITO plate was used as the cathode and the PBS solution containing RBC was used as the electrolyte, which was filled into the 10-mm-diameter × 10 mm cylindrical center hole, and O_2 gas was supplied to the electrolyte by bubbling solution. The single cell performance was evaluated by slow rate current sweep techniques on Solartron SI1287 Electrochemical Interface.

3. Results and discussion

3.1. Observation of RBC in PBS solution by confocal laser scanning microscopy and UV-vis spectroscopy

The morphology of RBCs on the ITO electrode was observed by a confocal laser scanning microscopy (CLSM). Figure S2 shows a superposed image of the optical and fluorescence images of RBCs in the PBS solution on the bare ITO electrode observed by the CLSM. The diameter and the height of one RBC were approximately 8 μmϕ and 2 μm, respectively, and its own hollow spheres were observed. Thus, the RBCs good

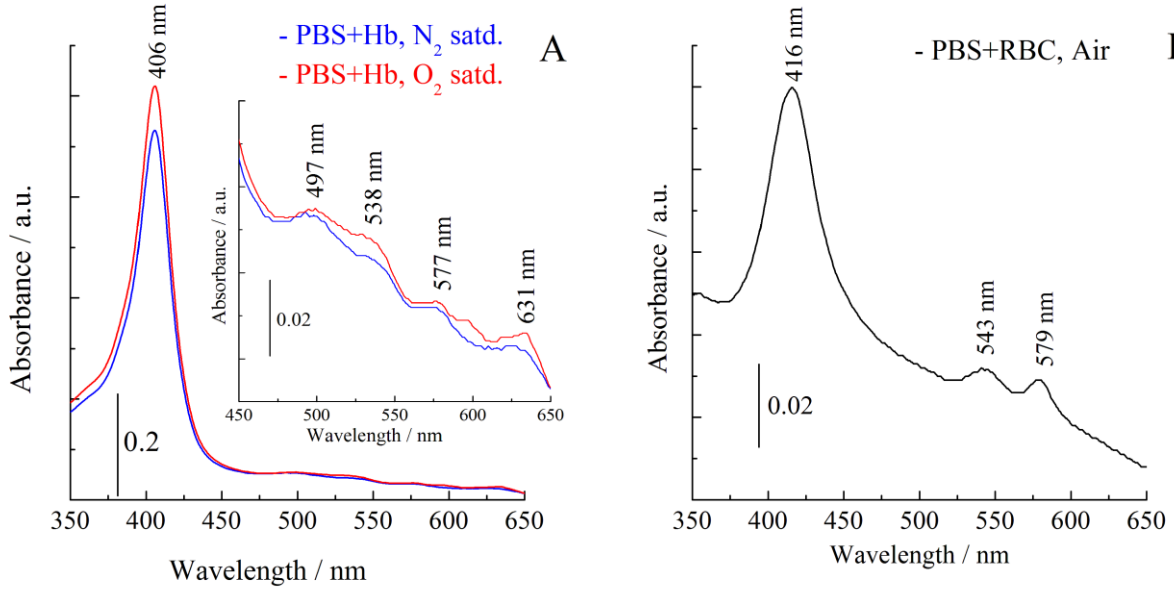

Figure 1. UV-vis transmission spectra of bovine Hb and human RBC in PBS solutions. The solution of bovine Hb was deaerated with N_2 or O_2 saturated by bubbling gas and that of human RBC was under air atmosphere.

retained their native configuration in blood in the PBS solution on the bare ITO electrodes. Figure 1 shows the UV-vis transmission spectra observed in the PBS solution containing human Hb in RBC and bovine Hb. The heme Fe in Hb can be classified at least into following three states. DeoxyHb and oxyHb containing the heme Fe(II) are O_2 unbound and bound Hb, respectively, and can work as O_2 carrier in vivo. MetHb containing heme Fe(III) is typically formed by auto-oxidation in vivo and shows no functions for O_2 carrier. It is well-known that these Hb molecules display different UV-vis spectra. In bovine Hb containing solution as shown in Fig. 1A, Soret band was observed at 406 nm and four weak peaks at 497, 538, 577, and 631 nm appeared in the Q-band region. These bands are similar to those for the met-Hb in a neutral pH solution (Pietri et al., 2005). The observed all bands were almost identical even in the O_2 saturated PBS solution containing Hb, indicating no O_2 binding function for bovine Hb in the PBS solution. These results prove that the Hb species in the PBS solution are metHb molecules. On the other hand, Soret band of 416 nm, β band of 543 nm, and α band of 579 nm due to oxyHb (Dewilde et al., 2006) were clearly observed in human Hb in RBC under air atmosphere as shown in Fig. 1B. These results indicated that the phospholipid bilayer membrane of RBCs protected the native environment around Hb.

3.2. Electrochemical evaluation for direct electron transfer be-tween RBCs and ITO electrodes.

Figure 2 shows the CV curves observed with the sweep rate, ν, of 0.5 V s^{-1} at the bare ITO electrode in the PBS solutions containing and not containing RBC. A pair of well-defined redox peaks was observed at around -0.08_9 and -0.21_5 V in the PBS solution containing RBC. The formal potential, $E°'$, of heme Fe(II)/Fe(III) couple of Hb in RBC was estimated to be -0.15_2 V taken at the midpoint of redox peaks. It good corresponds to that of bovine Hb in our previous work (Ayato et al., 2007). Thus, these results reveal that Hb molecules in RBCs exhibit the DET activity on the bare ITO electrodes without via any mediators such as transmembrane proteins in phospholipid bilayer membrane of RBC. A Hb entrapped in didodecyldimethylammonium bromide (DDAB) film, which is a kind of lipid, deposited on glassy carbon shows the $E°'$ of -0.25 V vs. saturated calomel electrode (SCE) in a PBS + 50 mM NaBr (pH 7.4) solution (Mimica et al., 2001). These results suggested that the phospholipid bilayer membrane of RBC itself and the ITO electrode would bring about the positive formal potential of *ca.* 56 mV.

The quantity of electrochemically active Hb molecules can be calculated from the integration of the charge, Q, in CVs by using the equation of $Q = nFA\Gamma^*$, where n is the number of electron transferred per protein molecule, F is Faraday constant, A is the surface area of the electrode, and Γ^* is concentration of the protein molecule. The quantity of the monolayer deposition of Hb molecules can be estimated to be 8.3×10^{-12} mol cm^{-2}, assuming one molecule occupied 20 nm^2. It was surprising that the estimated quantity of electrochemically active Hb molecules in human RBC from CVs was approximately 3.0×10^{-11} mol cm^{-2}, assuming the number of electron for one Hb molecule having four iron-bearing heme groups is 4, whereas that of

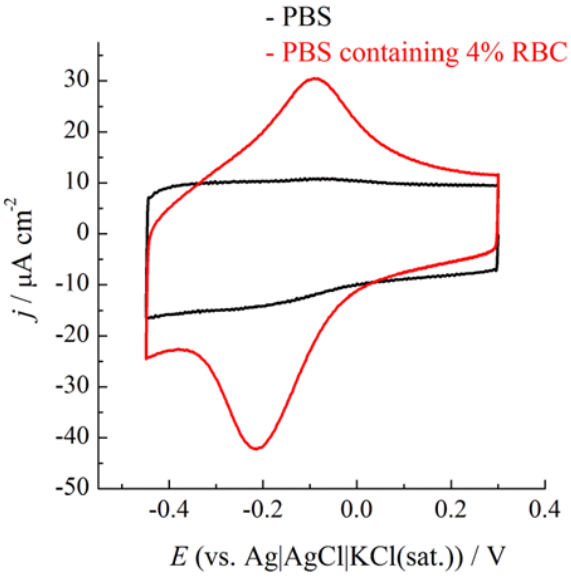

Figure 2. CVs of ITO electrodes in 39 mM PBS (pH 7.4) and PBS solution containing 4%(m/m) RBC. Sweep rate is 0.5 V s^{-1}.

bovine Hb was approximately monolayer or less monolayer deposition in our previous study (Ayato et al., 2007). A similar result is reported using Hb in RBCs from fish blood on a glassy carbon electrode (Xu et al., 2008). Scheller et al., 2005 reported that a much higher charge is transferred at one mercury drop than corresponds to the reduction of one Hb monolayer. The obtained results indicate either a very rapid exchange of Hb molecules in RBC at the vicinity of the electrode surface or the charge transfer through several Hb molecules in RBC. Consequently, phospholipid bilayer membrane of RBC would show some promoting effects, such as protection from denaturation due to adsorption of proteins onto the electrodes, for the electron transfer of Hb with the bare ITO electrode.

The CV curves were recorded with different sweep rates from 0.01 to 1.0 V s^{-1} in the PBS solutions containing and not containing RBC at the bare ITO electrode. The CV peak currents were determined by subtracting the current value in the PBS solution only at the same electrode potential, i.e. non-Faradaic current, from the peak current observed in the PBS solution containing RBC as shown in Fig. S3. When the peak current was plotted against sweep rate as shown in Fig. 3, liner relationship was obtained both of anodic, $j_{p,a}$, and cathodic, $j_{p,c}$, peak current densities. It is well-known that the peak current of CV is proportional to the sweep rate in the surface-controlled electrode process (Bard and Faulkner, 2001). Additionally, the plots of log $j_{p,a}$ and log v in Fig. S4 showed the linear relationship. The slope of it is known to be obtained 0.5 when the electrode reaction is ideal diffusion-controlled electrode process, while ideal surface-controlled electrode process displays the slope of 1 (Han et al., 2002; Murray, 1984). The slope obtained from Fig. S4 was 0.94. These results prove that the electron transfer between Hb in RBC and the bare ITO electrode surface is almost the surface-controlled electrode process, while RBC would not be strongly adsorbed on the ITO electrode surface as discussed later, i.e. in Fig. S6.

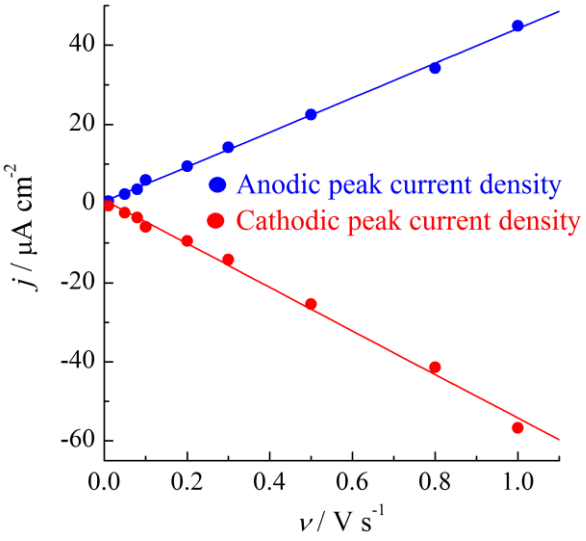

Figure 3. Dependence on the sweep rate against the peak current.

The electron transfer rate constant, k_s, of Hb in RBC at the ITO electrode can be estimated from diffusionless CV curves based on Laviron's methods (Laviron, 1979). The CV curves were also recorded with the sweep rates until 10 V s^{-1} to be obtained the difference of the peak potential, ΔE_p, > 200/n mV where the number of electron transferred per one heme Fe(II)/Fe(III) in Hb is 1. Figure S5 shows the plots of E_p against log v. The values of ΔE_p larger than 200 mV were obtained from 5 to 10 V s^{-1}, and linear regression were made for the anodic, $E_{p,a}$, and the cathodic, $E_{p,c}$, peak potentials between 5 and 10 V s^{-1}. The transfer coefficient, α, was estimated from the slope of linear regression lines equal to -2.3 $RT/\alpha n$F for $E_{p,c}$ and -2.3 $RT/(1-\alpha)n$F for $E_{p,a}$, where R is gas constant and T is temperature, and obtained to be 0.53 from $E_{p,a}$ and 0.47 from $E_{p,c}$. The results of α were near 0.5, and the intersection of the linear regression lines showed -0.153 V, which was near the formal potential determined above. The k_s was determined from the equation of $\log k_s = \alpha\log(1-\alpha) + (1-\alpha)\log \alpha - \log(RT/n\mathrm{F}v) - \alpha(1-\alpha)n\mathrm{F}\Delta E_p/2.303RT$ when $n\Delta E_p$ > 200 mV. The obtained value of k_s was 11.9 $s^{-1} \pm 0.4$.

The diffusionless CV curves are often associated with the adsorption of reactants on the electrode surfaces. In this study, the PBS solution containing RBC in the electrochemical cell was exchanged with the PBS solution for

ten times and the CV measurements were carried out with the sweep rate of 0.8 V s^{-1} in the PBS solution. The results are shown in Fig. S6. The redox peak current dramatically decreased after exchanging with the PBS solution until 5 times, and definable redox peaks were hardly observed in the PBS solution exchanged for ten times. These results indicate that RBCs are not strongly adsorbed on the bare ITO electrode. It is favorable if the RBC-ITO cathode is prepared in the blood vessel and applied as the body implantable power supplies because RBCs can probably be easily exchanged with fresh RBCs on the ITO electrode surface by blood flow.

The CV measurements were also performed in O_2 saturated PBS solution containing RBC. The results are shown in Fig. 4. The large reduction current increased from around -0.15 V and reached to over 100 μA cm^{-2} at -0.45 V, while such reduction current was not observed in the dearated PBS solution containing RBC and O_2 saturated PBS solution not containing RBC. These results prove that the Hb molecules in RBC show the DET activity and the electrocatalytic activity for the oxygen reduction reaction (ORR) on the bare ITO electrode. These findings are great advantages for practical use of ITO electrodes with RBC to BFCs cathode, since the system can operate by simply inserting the bare ITO electrodes into the blood vessel without any purification, immobilization, and modification of the enzymes onto the electrodes and gas supply systems.

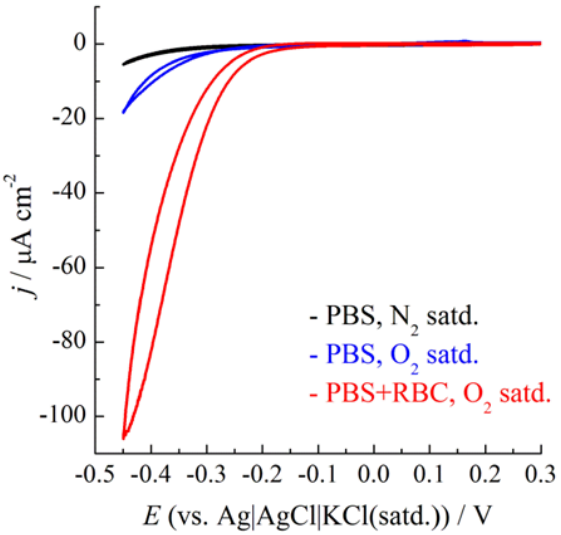

Figure 4. CVs of ITO electrodes in N_2 and O_2 saturated PBS solution containing not containing 4% RBC. Sweep rate is 0.01 V s^{-1}.

Performance of biofuel cells with RBC-ITO cathodic systems. The onset potential, E_{on}, of ORR was observed around -0.15 V in the O_2 saturated PBS solution containing RBC at the bare ITO electrode as mentioned above. On the other hand, Nernstian electrode potential of the H_2 oxidation is -0.64 V vs. Ag|AgCl|KCl(satd.) in pH 7.4. Hence, it can be expected to obtain the open-circuit voltage (OCV) value of *ca.* 0.5 V when the cathode, the anode, and the electrolyte are composed of the O_2|RBC|ITO, the H_2|Pt/C, and the PBS solution, respectively, on the assembled single cell of BFCs.

Figure 5 shows the *I-V* and the power characteristics recorded with the sweep rate of 50 nA s^{-1} on the assembled single cell. The observed OCV was 0.43 V. This value is lower than that of the expectation. In this single cell, the electrolyte was saturated with O_2 by bubbling electrolyte solution; thus, it is most likely that the cross-over phenomena of O_2 to the anode resulted in the mixed potential of the electrode. The maximum current and power densities were obtained at around 11.3 μA cm^{-2} and 0.68

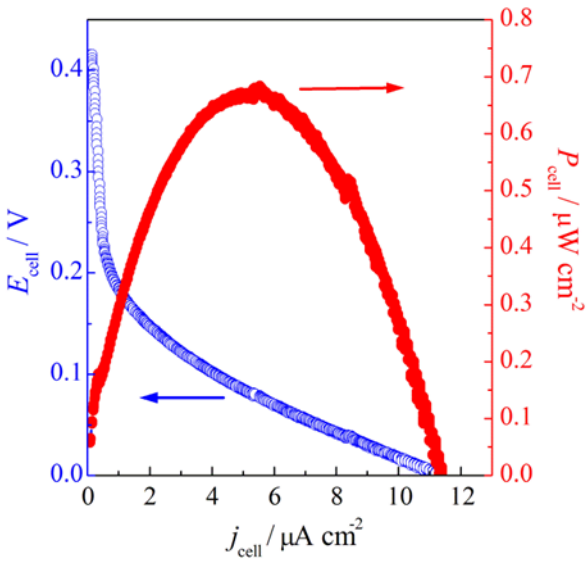

Figure 5. *I-V* and power characteristics on the single cell composed of O_2|RBC|ITO cathode and H_2|Pt/C anode. Sweep rate is 50 nA s^{-1}.

μW cm^{-2}, respectively, while the cardiac pacemaker generally sends < 10 μA signal to heart. Consequently, we successfully demonstrated that the BFC utilizing RBC as the cathode electrocatalysts could operate under this experimental condition. From the CV curve recorded in O_2 saturated PBS solution, better single cell performances would be expected by improving the cell construction and the assembling technique. A further study on this is in progress.

4. Conclusions

Red blood cells (RBCs) from human showed electron transfer activity with indium tin oxide (ITO) electrodes. Active species for the electron transfer in RBCs were probably hemoglobin (Hb) molecules encapsulated by their phospholipid bilayer membrane. According to the definition of electron path way between direct electron transfer (DET) and mediated electron transfer (MET) on the electrode surface, we concluded that the observed electron transfer was classified into the DET-type electrode since an individual natural cell without any exogenous treatments showed the electron transfer directly with the electrodes. Analyses of cyclic voltammetric (CV) data observed with different sweep rate disclosed that the electron transfer was almost dominated by the surface-controlled electrode process, whereas RBCs were not strongly adsorbed on the ITO electrode surface. In addition, Hb molecules in RBCs showed oxygen reduction reaction (ORR) activity based on DET with the ITO electrode. The open-circuit voltage and the maximum power density were observed at 0.43 V and 0.68 μW cm^{-2}, respectively, on the single cell composed of the O_2|RBC|ITO cathode and the H_2|Pt/C anode.

Supplemental Information: Illustration of single cell components (Fig. S1), Confocal laser scanning microscopic image of RBCs in PBS solution on bare ITO electrode (Fig. S2), CVs of ITO electrodes with deferent sweep rates in 39 mM PBS (pH 7.4) solution containing 4%(m/m) RBC. Sweep rates are indicated in the figure (Fig. S3), Dependence of log *j* on log *v* (Fig. S4), Variations of anodic and cathodic peak potential as a function of logarithm sweep rate (Fig. S5), CVs of ITO electrodes in PBS solution containing 4%(m/m) RBC before and after exchanging with PBS solution. Sweep rate is 0.8 V s^{-1} (Fig. S6).

References

Ayato, Y.; Matsuda, N., 2009. Chem. Lett. 38, 504.

Ayato, Y.; Takatsu, A.; Kato, K.; Matsuda, N., 2008. Jpn. J. Appl. Phys. 47, 1333.

Ayato, Y.; Itahashi, T.; Matsuda, N., 2007. Chem. Lett. 36, 406.

Ayato, Y.; Kunimatsu, K.; Osawa, M.; Okada, T., 2006. J. Electrochem. Soc. 153, A203.

Ayato, Y.; Okada, T.; Yamazaki, Y., 2003. Electrochemistry 71, 313.

Bard, A. J.; Faulkner, R. F., 2001. Electrochemical Methods: Fundamentals and Applications, 2nd ed. John Wiley & Sons, Inc., New York.

Brunel, L.; Denele, J.; Servat, K.; Kokoh, K. B.; Jolivalt, C.; In-nocent, C.; Cretin, M.; Rolland, M.; Tingry, S., 2007. Biochem. Commun. 9, 331.

Bullen, R. A.; Arnot, T. C.; Lakeman, J. B.; Walsh, F. C., 2006. Biosens. Bioelectron. 21, 2015.

Cai, C.-J; Xu, M.-W.; Bao, S.-J.; Lei, C.; Jia, D.-Z., 2012. RSC Adv. 2, 8172.

Chen, C.-C.; Do, J.-S.; Gu, Y., 2009. Sensors 9, 4635.

Ci, Y.–X.; Li, H.–N.; Feng, J., 1998. Electroanalysis 10, 921.

Dewilde, S.; Ebner, B.; Vinck, E.; Gilany, K.; Hankeln, T.; Burmester, T.; Kreiling, J.; Reinisch, C.; Vanfleteren, J. R.; Kiger, L.; Marden, M. C.; Hundahl, C.; Fago, A.; Doorslaer, S. V.; Moens, L., 2006. J. Biol. Chem. 281, 5364.

Drobov, R.; Kurth, D. G.; Möhwald, H.; Scheller, F.W.; Lisdat, F., 2008. Angew. Chem. Int. Ed. 47, 3000.

Feng, J.-J.; Xu, J.-J.; Chen, H.-Y., 2006. Electrochem. Commun. 8, 77.

Gorton, L.; Lindgren, A.; Larsson, T.; Munteanu, F. D.; Ruzgas, T.; Gazaryan, I., 1999. Anal. Chim. Acta 400, 91.

Gu, H.–Y.; Yu, A.–M.; Chen, H.–Y., 2001. J. Electroanal. Chem. 516, 119.

Halámková, L.; Halámek, J.; Bocharova, V.; Szczupak, A.; Al-fonta, L.; Katz, E., 2012. J. Am. Chem. Soc. 134, 5040.

Han, X.; Cheng, W.; Zhang, Z.; Dong, S.; Wang, E., 2002. Biochim. Biophys. Acta 1556, 273.

Laviron, E., 1979. J. Electroanal. Chem. 101, 19.

Ikeda, T.; Kano, K., 2003. Biochim. Biophys. Acta 1647, 121.

Jia, Y.; Wood, F.; Menu, P.; Faivre, B.; Caron, A.; Alayash, A. I., 2004. Biochim. Biophys. Acta 1672, 164.

Jones, E. M.; Balakrishnan, G.; Spiro, T., 2012. J. Am. Chem. Soc. 134, 3461.

Kafi, A. K. M.; Crossley, M. J., 2013. Biosens. Bioelectron. 42, 273.

Kang, X; Wang, J.; Wu, H.; Aksay, I. A.; Liu, J.; Lin, Y., 2009. Biosens. Bioelectron. 25, 901.

Katz, E.; Willner, I.; Kotlyar, A. B., 1999. J. Electroanal. Chem. 479, 64.

Kawahara, N. Y.; Ohno, H., 1998. Electrochim. Acta 43, 1493.

Mimica, D.; Ringuedé, A.; Agurto, C.; Bedioui, F.; Zagal, J., 2004. Electroanalysis 19, 16.

Mimica, D.; Zagal, J. H.; Bedioui, F., 2001. J. Electroanal. Chem. 497, 106.

Murray, R. W.; in: Bard, A. J. (Ed.), Electroanalytical Chemistry, vol.13, Marcel Dekker, New York, 1984, p. 191.

Nazaruk, E.; Smoliński, S.; Swatko-Ossor, M.; Ginalska, G.; Fiedurek, J.; Rogalski, J.; Bilewicz, R. 2008. J. Power Sources 183, 533.

Palmore, G. T. R.; Bertschy, H.; Bergens, S. H.; Whitesides, G. M., 1998. J. Electroanal. Chem. 443, 155.

Perutz, M. F.; Muirhead, H.; Cox, J. M.; Goaman, L. C. G.; Mathews, F. S.; McGandy, E. L.; Webb, L. E., 1968. Nature 219, 29.

Pietri, R.; Granell, L.; Cruz, A.; Jesús, W. D.; Lewis, A.; Leon, R.; Cadilla, C. L.; Garriga, J. L., 2005. Biochim. Biophys. Acta 1747, 195.

Prakash, P. A.; Yogeswaran, U.; Chen, S.-M., 2009. Sensors 9, 1821.

Rasmussen, M.; Ritzmann, R. E.; Lee, I.; Pollack, A. J.; Scherson, D., 2012. J. Am. Chem. Soc. 134, 1458.

Revenga-Parra, M.; Lorenzo, E.; Pariente, F., 2005. Sens. Actuat. B 107, 678.

Scheller, F. W.; Bistolas, N.; Liu, S.; Jänchen, M.; Katterle, M.; Wollenberger, U., 2005. Adv. Colloid Interface Sci. 116, 111.

Shan, D.; Han, E.; Xue, H.; Cosnier, S., 2007. Biomacromolecules 8, 3041.

Shi, G.; Sun, Z.; Liu, M.; Zhang, L.; Liu, Y.; Qu, Y.; Jin, L., 2007. Anal. Chem. 79, 3581.

Sun, H.; Hu, N., 2004. Biophys. Chem. 110, 297.

Tarasevich, M. R.; Bogdanovskaya, V. A.; Kapustin, A. V., 2003. Electrochem. Commun. 5, 491.

Togo, M.; Takamura, A.; Asai, T.; Kaji, H.; Nishizawa, M. 2008. J. Power Sources 178, 53.

Topoglidis, E.; Astuti, Y.; Duriaux, F.; Grätzel, M.; Durrant, J. R., 2003. Langmuir 19, 6894.

Tsujimura, S.; Fujita, M.; Tatsumi, H.; Kano, K.; Ikeda, T., 2001. Phys. Chem. Chem. Phys. 3, 1331.

Yong, Y-C.; Dong, X.-C.; Chan-Park, M. B.; Song, H.; Chen, P., 2012. ACS Nano 6, 2394.

Wang, Y.–H.; Guo, J.–W.; Gu, H.–Y., 2010. Microchim Acta 171, 179.

Xu, Y.; Hu, C.; Hu, S., 2008. Bioelectrochem. 72, 135.

Yin, F.; Shin, H.-K.; Kwon, Y.-S., 2005. Biosens. Bioelectron. 21, 21.

Zebda, A.; Renaud, L.; Cretin, M.; Innocent, C.; Pichot, F.; Fer-rigno, R.; Tingry, S., 2009. J. Power Sources 193, 602.

Zhao, G.; Xu, J.-J.; Chen, H.-Y., 2006. Electrochem. Commun. 8, 148.

Zhao, G.-C.; Xu, M.-Q.; Ma, J; Wei, X.-W., 2007. Electrochem. Commun. 9, 920.

Zhang, J.; Oyama, M., 2004. Electrochim. Acta 50, 85.

Zhou, Y.; Li, Z.; Hu, N.; Zeng, Y.; Rusling, J. F., 2002. Langmuir 18, 8573.

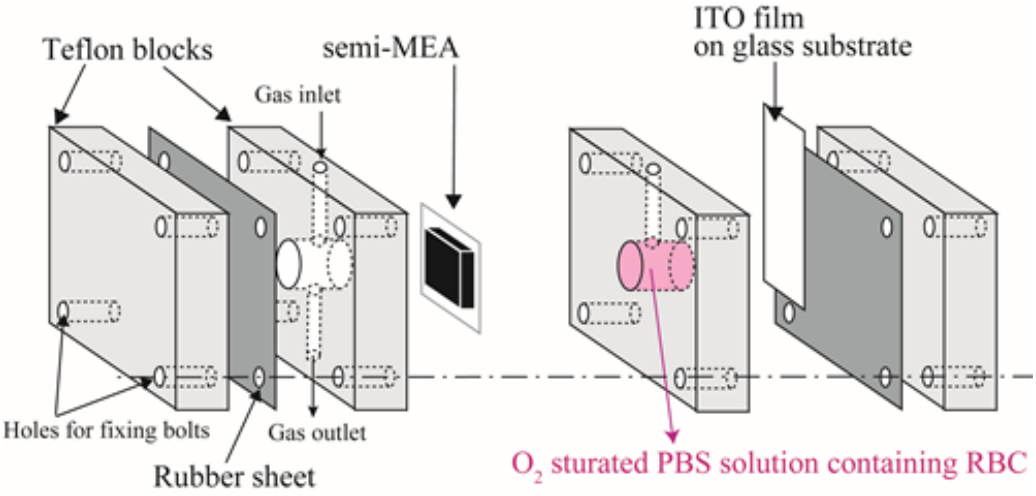

Figure S1. Illustration of single cell components.

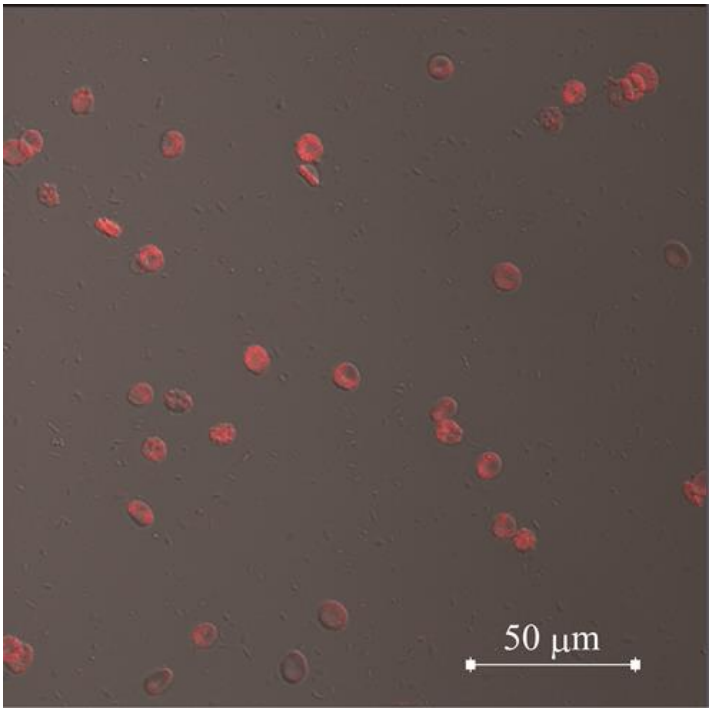

Figure S2. Confocal laser scanning microscopic image of RBCs in PBS solution on bare ITO electrode.

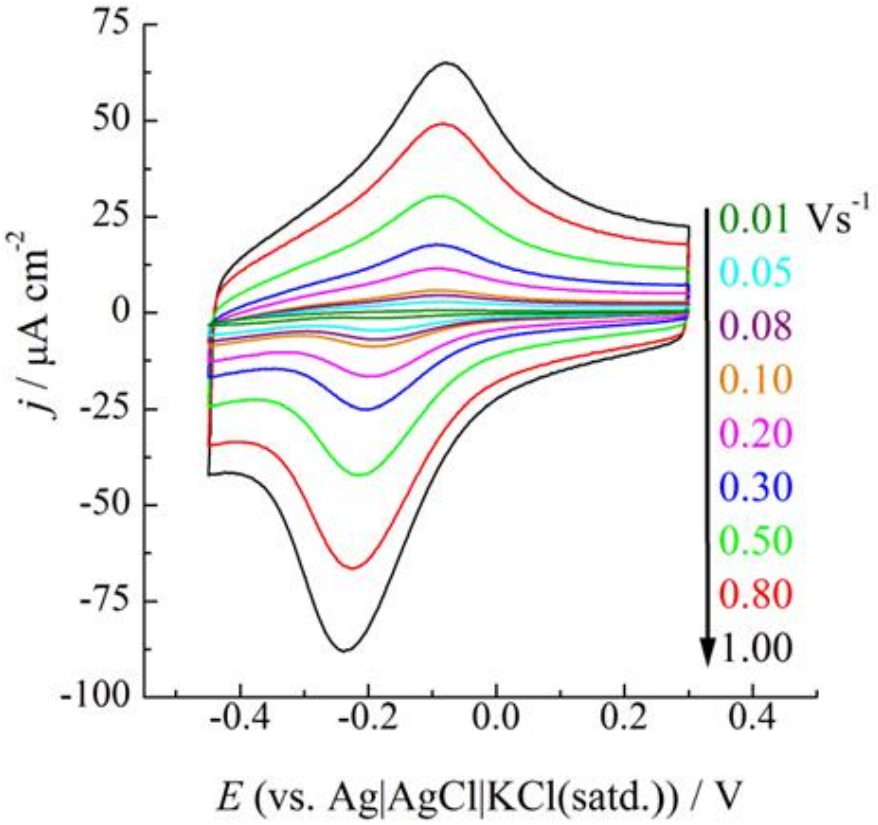

Figure S3. CVs of ITO electrodes with deferent sweep rates in 39 mM PBS (pH 7.4) solution containing 4%(m/m) RBC. Sweep rates are indicated in the figure.

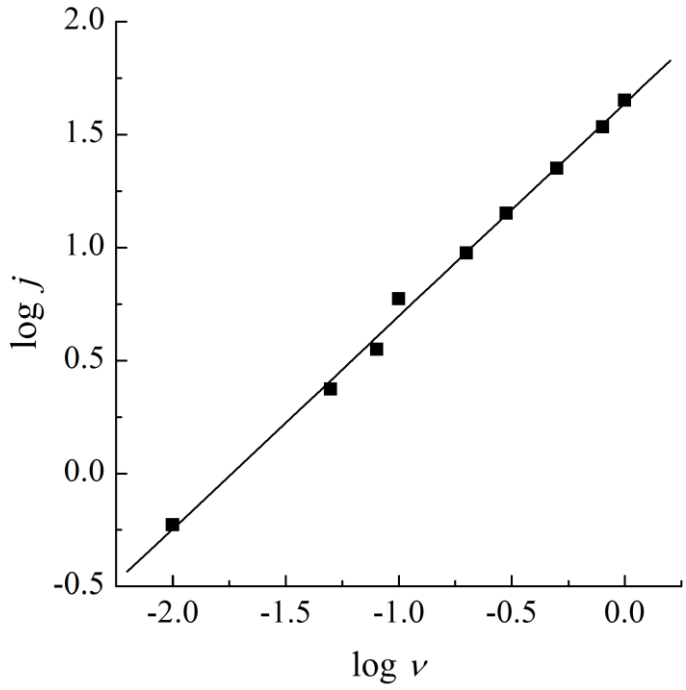

Figure S4 Dependence of log *j* on log *v*.

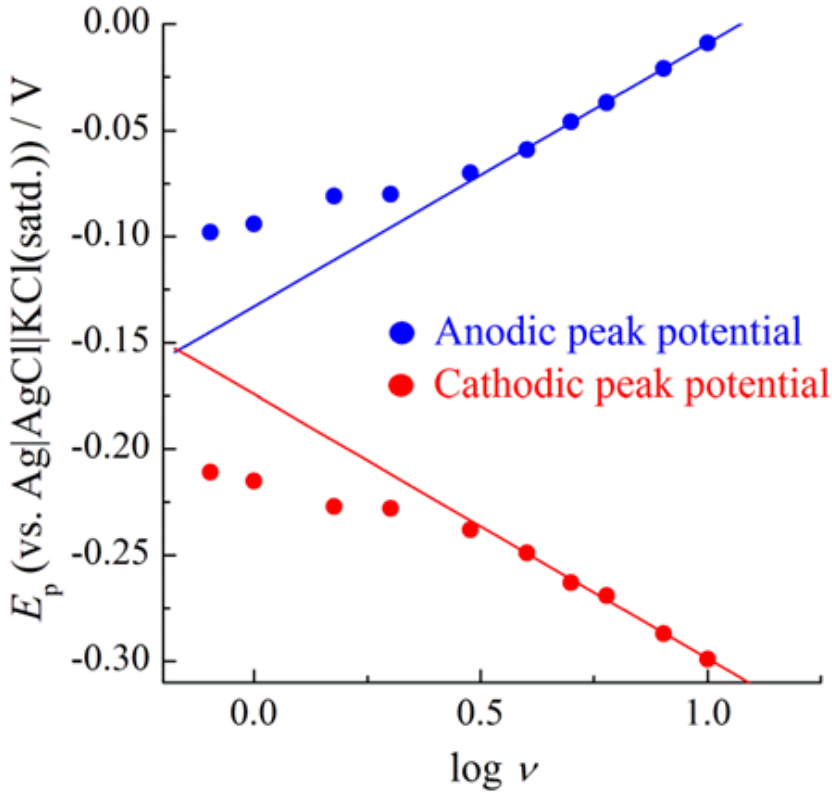

Figure S5. Variations of anodic and cathodic peak potential as a function of logarithm sweep rate.

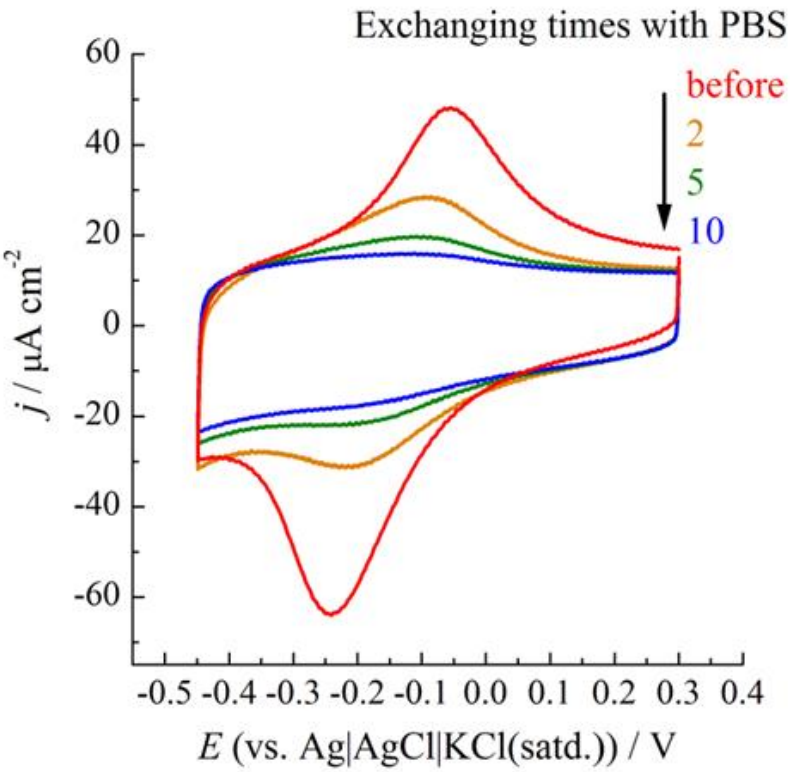

Figure S6. CVs of ITO electrodes in PBS solution containing 4%(m/m) RBC before and after exchanging with PBS solution. Sweep rate is 0.8 V s^{-1}.